Journal of Crystal Growth 347 (2012) 88–94

Contents lists available at SciVerse ScienceDirect

Journal of Crystal Growth

journal homepage: www.elsevier.com/locate/jcrysgro

Microstructure of epitaxial GaN films grown on chemomechanically polished GaN(0001) substrates

Li Huang [a,1], Fang Liu [a], Jingxi Zhu [a], Ranga Kamaladasa [a], Edward A. Preble [b], Tanya Paskova [b], Keith Evans [b], Lisa Porter [a], Yoosuf N. Picard [a], Robert F. Davis [a,*]

[a] Department of Materials Science and Engineering, Carnegie Mellon University, Pittsburgh, PA 15213, USA
[b] Kyma Technologies, Inc., Raleigh, NC 27617, USA

ARTICLE INFO

Article history:
Received 24 December 2011
Accepted 1 March 2012
Communicated by R. Kern
Available online 16 March 2012

Keywords:
A1. Grain boundary
A1. Substrate
A1. Terrace/step
A1. Threading dislocations
A3. Homoepitaxy
B1. GaN

ABSTRACT

An organometallic vapor phase epitaxy-based process route has been developed to achieve homoepitaxial deposition of GaN(0001) films via step-flow growth on substrates having $<1^\circ$ off-cut. Atomic force microscopy of the surfaces of 0, 1, 2, 5 and 10 nm thick films revealed steps and terraces as the only features; three-dimensional GaN islands were not observed. Film–substrate interfaces were not present in cross-sectional samples using high-resolution TEM. This indicated that continuous film growth occurred from steps on the substrate without re-nucleation and defect formation on the terraces. This process route also mitigated the generation of additional dislocations, as validated by the exact matches of the density and positions of dislocations that reached the substrate surface and those observed in a subsequently grown 600 nm film. The influence of grain boundaries in the interior of the GaN substrates was manifest in variations in terrace width and step orientation across the substrates and the films. A grain orientation map generated across a representative substrate revealed highly disoriented grains on the periphery. The disorientation angles between these adjacent grains were centered around $\sim35^\circ$, $\sim70^\circ$ and $\sim90^\circ$.

1. Introduction

Alloys of GaN, AlN and InN are the materials of choice for LEDs emitting within the commercially available wavelength range of approximately 240–540 nm. At present, the principal substrates on which these devices are commercially grown and fabricated are sapphire and silicon carbide (SiC) due to their stability in the high-temperature and hydrogen-containing growth environment as well as their availability. However, the significant differences in the lattice parameters and the coefficients of thermal expansion between these substrates and the initial nitride thin films in the device heterostructures over the temperature ranges of growth cause the introduction of very high densities of point defects at the substrate/film interface, dislocations that thread throughout the device and V-shaped defects that can form in the light-emitting multi-quantum well active region and top p-GaN cladding layer [1–10]. Additionally, stresses generated within the active region due to the growth of coherent quantum wells and barriers along [0001] impose a strong piezoelectric field that separates the electrons and holes in these wells and reduces the probability of radiative recombination and the associated internal quantum efficiency. All defects and the internal electric fields are detrimental to the performance of LEDs [10–14].

The availability and diameter of GaN substrates are slowly increasing and are currently used primarily for the growth of nitride-based blue- and green-emitting semiconductor lasers. Their use enables one to achieve films more closely matched in physical properties to GaN with diminished piezoelectric fields and markedly reduced densities of dislocations and other defects. Threading dislocations (TDs) have been observed to form randomly (a) at the outset of growth of and within the initial III-nitride "nucleation" layer deposited on sapphire substrates [4] and (b) from clusters of point defects at the SiC substrate/buffer layer interface [2,3]. Wu et al. [15] have reasoned that dislocations are also generated to accommodate stresses within tilt boundaries formed during the coalescence of three-dimensional GaN islands within the template layer subsequently grown on the nucleation layer on sapphire substrates. The clustering TDs at grain boundaries have been observed in transmission electron microscopy (TEM) [16–18] and electron channeling contrast imaging (ECCI) [19]. The reported densities of dislocations in the aforementioned studies are substantial; within the range of 10^8–10^{10} cm^{-2}. Thus, it is important for increased radiative recombination and the associated internal

* Corresponding author. Fax: +1 412 268 3113.
E-mail address: rfd@andrew.cmu.edu (R.F. Davis).
[1] Now with Soitec Phoenix Lab, Phoenix, AZ 85284, USA.

0022-0248/$ - see front matter © 2012 Elsevier B.V. All rights reserved.
http://dx.doi.org/10.1016/j.jcrysgro.2012.03.002

quantum efficiency that the mechanism of growth of any subsequent layer(s) on a GaN substrate be as a result of step-flow growth rather than the re-nucleation, lateral growth and coalescence of islands on the terraces of these substrates to avoid the simultaneous generation of TDs at the interface.

Xu et al. [20] reported that the morphology of undoped GaN films homoepitaxially grown via organometallic-vapor-phase-epitaxy (OMVPE) on GaN(0001) wafers (root-mean-square roughness (RMS) < 0.3 nm) produced by hydride vapor epitaxy (HVPE) was much smoother (RMS $= 0.39$ nm over a $10 \times 10\ \mu m^2$ area) than a similar film (RMS $= 0.91$ nm) grown on an [0001]-oriented GaN/sapphire template. The former films exhibited a parallel step structure; the latter contained a swirled step structure and a much higher density of step terminations. The optimized conditions were markedly different for growth on the two substrates (and also for growth on GaN/SiC templates). It was suggested that differences in either thermal conductivity or surface morphology or the arrangement of atomic steps accounted for the different conditions. Additional investigations by Xu et al. concerned with the homoepitaxial growth of (a) Si-doped, n-type and Mg-doped, p-type 3 μm thick GaN films on similarly oriented wafers and (b) both undoped and doped films on vicinal GaN(0001) wafers offcut 1°, 2°, 4° and 8° have also been reported [21]. Subsequent related investigations by Tachibana et al. [22] concerned with atomic force microscopy (AFM) and X-ray diffraction of GaN homoepitaxial layers grown on HVPE, n-type GaN(0001) substrates off-cut 0.2° towards $[1\bar{1}00]$ and $[11\bar{2}0]$ revealed the formation of a smooth morphology only on the surface of the former layer.

To date, very few investigations concerned with the determination of (a) the earliest stages of growth of GaN on GaN(0001) substrates and the generation of TDs [23], (b) the growth mode of GaN on these substrates and (c) the evolution of the surface microstructure of the GaN films as a function of thickness have been reported. The investigations herein have addressed these issues via microstructural characterization of the surfaces and cross-sections of HVPE-grown, on-axis, [0001]-oriented and chemo-mechanically polished (CMP) substrates and 1 nm, 2 nm, 5 nm, 10 nm and 600 nm thick GaN(0001) films grown on these wafers via OMVPE. AFM results of the surfaces of films grown using our optimized process route revealed a step-and-terrace surface microstructure without three-dimensional island formation, which indicated that step-flow was the operative mode of growth. Electron microscopy did not reveal a film/substrate interface. Correspondence between the TDs in the 600 nm film with those in the substrate confirmed that no additional defects were generated, as also inferred by the film growth mechanism. Finally these studies identified the variation of step orientation and terrace width of the film surface as a result of the existence of multi-grains carried over from the substrate.

2. Experimental details

Free-standing, 1 cm $(L) \times 1$ cm $(W) \times 0.45$ mm (H), CMP GaN(0001) substrates (RMS < 0.5 nm) off-cut within 1° towards $[1\bar{1}00]$ were obtained from Kyma Technologies, Inc. [24]. The off-cut angle is one of the important parameters that determine the growth mode of any subsequently deposited layer; thus, all GaN(0001) substrates in this study were intentionally chosen to have the same measured off-cut angle of $0.17 \pm 0.02°$.

The homoepitaxial growth of the GaN(0001) films was achieved via OMVPE in a vertical, resistively heated, cold wall, pancake-style system. Prior to loading into the reactor, each GaN substrate was cleaned ultrasonically and sequentially in acetone, methanol and isopropanol for 5 min in each solvent, submersed in a warm HCl solution for 10 min, rinsed in de-ionized water and dried in flowing N_2. The reactor chamber was evacuated to 7×10^{-6} Torr. Nitrogen was flowed along the quartz chamber wall (4.5 slm) to avoid coating formation and over the graphite-heating element (0.5 slm) to prevent reaction with ammonia. Each substrate was heated to 800 °C within 10 min in a flowing mixture of 3 slm NH_3 and 4 slm H_2 at a total pressure of 20 Torr and annealed at this temperature for 5 min to remove the hydrocarbon and native oxide films from the surface [25]. This in-situ thermal cleaning processing is important to avoid the generation of new TDs at the homoepitaxial film/substrate interface [23]. Triethylgallium (TEG) (carried in H_2) was then introduced into the chamber at a flow rate of 25.3 μmol/min, and growth of the GaN films initiated. The flow rates of NH_3 and H_2 and the total pressure were maintained at the same values noted above.

As indicated in the previous section, the early stages of GaN homoepitaxial growth must be carefully controlled to avoid island formation, lateral growth and coalescence, and the simultaneous generation of TDs at the boundaries. The temperature was then ramped to individual temperatures between 800 °C and 1000 °C at a rate of 3.3 °C/s, and the flow rate of TEG increased simultaneously and linearly as a function of time from 25.3 μmol/min at a rate of 1.265 μmol/min/s. This low temperature range was employed to mitigate nitrogen evaporation from both the substrates and the growing films and the concomitant formation of Ga droplets.

Companion studies in our laboratory have shown that the growth rate of GaN within the temperature range of 800–1000 °C is controlled solely by the TEG flow rate, i.e., increasing the temperature within this range does not affect the growth rate. This indicates that the OMVPE system was operated in a mass-transport limited-growth regime during the growth of the GaN films. That is, the growth rate of the films was dependent on the transport of the reactant gases to the surface, and the composition and uniformity of the films were controlled by the reactor geometry and flow conditions [26]. A linear relationship of the growth rate of GaN film with the TEG flow rate was established in a prior research in our laboratory. As such, the thickness of each GaN film could be and was determined by the integration of growth rate over the time of a particular deposition. The investigation involved the separate growths of 1 nm, 2 nm, 5 nm and 10 nm GaN films on GaN substrates. These values of film thickness correspond to growth times of 7 s, 12 s, 24 s and 39 s, respectively, that began at the outset of the increase in TEG flux. The individual final temperatures were 823 °C, 840 °C, 880 °C and 930 °C, respectively. The flow of TEG was stopped at the end of each growth period, while the flow rates of H_2, NH_3 and N_2 were maintained during cooling over a period of three minutes. The surfaces of the as-grown GaN films were characterized via AFM in tapping mode. The GaN film/GaN substrate interface was evaluated via high-resolution cross-section TEM.

For a GaN film having thickness of 600 nm on a GaN substrate, growth continued at 1000 °C and TEG flow rate of 101.2 μmol/min following the ramp of both temperature and TEG flow rate. The location and density of the threading dislocations that intersected the surface of the GaN(0001) substrate were identified and mapped prior to layer growth using ECCI in a scanning electron microscope (SEM) equipped with a backscatter detector. The details of this technique for dislocation characterization are available in Refs. [19,27]. The areas on the surface of the GaN substrate where the ECCI images were acquired were delineated with cross-shaped markers using focused ion beam (FIB) etching in a Nova 600 Dual-Beam (electron and focused-ion) system. These markers were mimicked in the subsequently grown 600 nm GaN film. The surface of this film was then etched in a

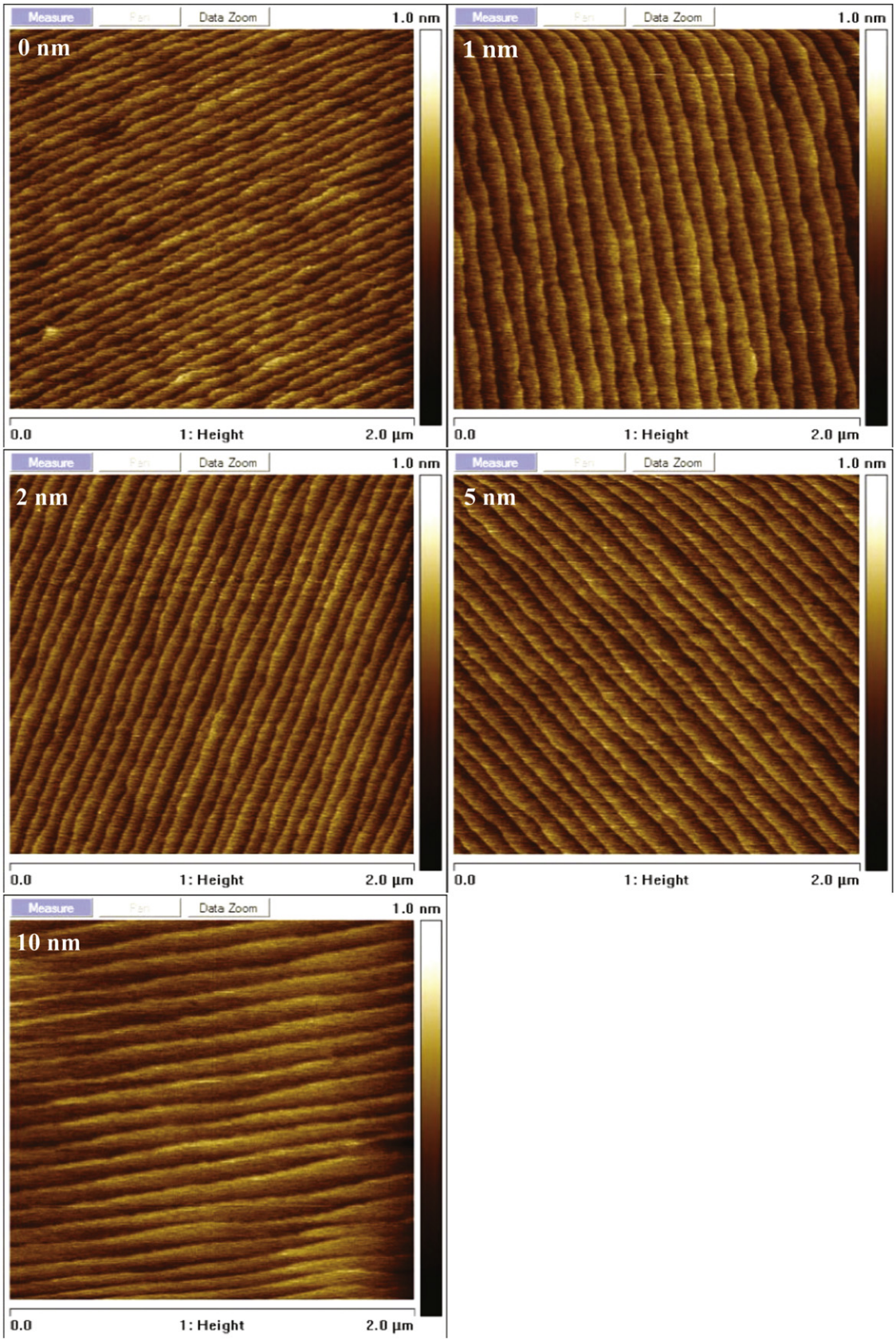

Fig. 1. Representative micrographs of the surfaces of a thermally annealed GaN(0001) substrate and of 1 nm, 2 nm, 5 nm, and 10 nm thick homoepitaxial GaN films. Each value of film thickness was achieved using linear ramps of temperature from 800 °C at a rate of 3.3 °C/s and TEG flow rate from 25.3 μmol/min. The individual final temperatures and TEG flow rates for the respective films were 823 °C and 34.155 μmol/min (1 nm), 840 °C and 40.48 μmol/min (2 nm), 880 °C and 55.66 μmol/min (5 nm), and 930 °C and 74.635 μmol/min (10 nm).

molten KOH solution containing 10 wt% MgO at 360 °C for 10 min [28]. The location and density of the threading dislocations in the delineated area of the GaN film were imaged in SEM.

An electron backscatter diffraction (EBSD) map of the highly disoriented grains in a representative GaN substrate was generated from data collected using an EDAX-TSL Hikari high-speed camera attached to the Dual-Beam system. Data collection was controlled using TSL OIM Data Collection v5.21 software. The backscattered diffraction patterns were obtained using an accelerating voltage of 25 kV at 9.8 nA. Orientation data was collected across the sample with a resolution of 20 μm. At each point, the orientation of the crystal lattice of the grain with respect to an arbitrary reference frame was represented in three "Euler angles". The aforementioned software expressed the "misorientation" of two grains in an angle–axis pair convention. The software acquired the orientation information (Euler angles) of the two neighboring grains and returned the smallest value of all possible rotation angles. This minimum rotation angle is known as the "disorientation angle". The EBSD map was then cropped and the poorly indexed points were removed using the grain dilation procedure in the software, a disorientation angle $>5^\circ$ was used to distinguish these grains from those observed in the AFM study. A histogram of the large disorientation angles was generated at intervals of 5°.

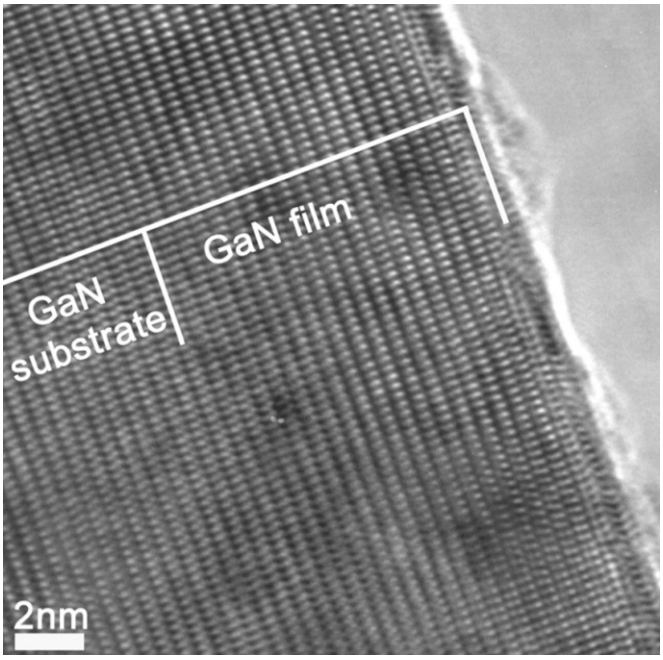

Fig. 2. High-resolution cross-sectional TEM image acquired along the [11$\bar{2}$0] zone axis of the 10 nm GaN film/GaN(0001) substrate sample. The line indicating the interface was determined from the knowledge of the thickness of the film from prior studies of the rate of growth and the length of each unit cell along [0001].

3. Results and discussions

The representative AFM micrographs shown in Fig. 1 reveal the surfaces of a thermally annealed GaN(0001) substrate and those of the 1 nm, 2 nm, 5 nm, and 10 nm thick GaN films grown on these substrates. Thermal damage, i.e., decomposition accompanied by nitrogen evaporation and the formation of Ga droplets, did not occur on the surface of the GaN substrates during the annealing step. A step-and-terrace microstructure replicating that of the surface of the underlying substrates was formed at the outset of the growth of each film. Three-dimensional GaN islands were not observed on any GaN film. These results indicate that step-flow was initially and continued to be the operative mode of growth. The following paragraphs describe the evolution of the microstructure and its interconnection with that of the substrate.

The cross-sectional, high resolution TEM image shown in Fig. 2 of the 10 nm film on a GaN substrate is representative of all the thin film/substrate samples in that the growth of the film was continuous from the GaN substrate and that no interface was observed. More importantly, the growth of the GaN film did not involve re-nucleation and the formation of extended defects at the interface between the film and the substrate. These results are in agreement with those acquired in the AFM investigations described above.

The continuation of the step/terrace microstructure of the GaN substrate by step-flow growth and the absence of three-dimensional island formation should mitigate or at least inhibit the formation of new threading dislocations. To test this hypothesis, an investigation concerned with the determination and comparison of the densities of threading dislocations in the GaN(0001) substrate and in the as-grown films was performed, as described in the previous section. The dislocations on the substrate are shown in the ECCI micrograph in Fig. 3(a). The larger contrast features, or spots, indicated by arrows are screw- and/or mixed-type dislocations, while the smaller spots indicated by circles are edge-type dislocations. Such delineation of GaN TD type based on

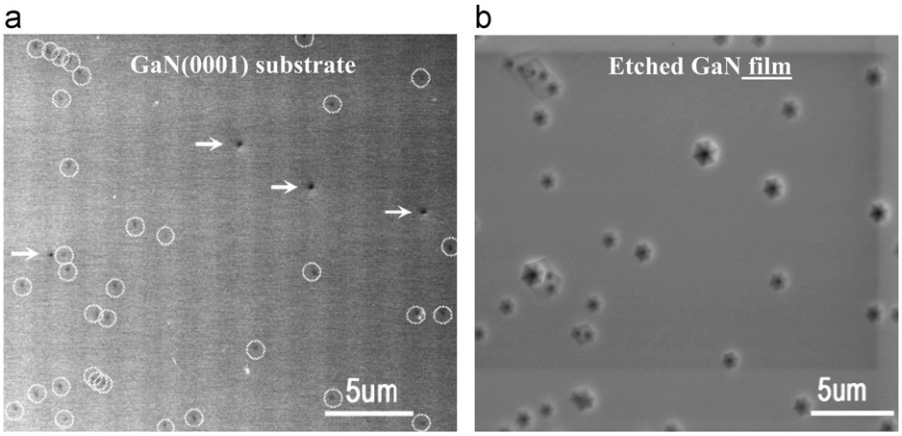

Fig. 3. (a) ECCI image of a GaN(0001) substrate. Larger ECCI contrast features denoted by arrows are screw-and/or mixed-type dislocations. Smaller size features indicated with circles are edge-type dislocations. (b) Chemically etched surface of a 600 nm GaN film grown on the substrate shown in (a). Both images were taken from the same region via reference to two focused ion-beam etched fiducial markers on the substrate surface and reproduced in the film, but located outside the micrographs. Note the 1:1 correspondence between dislocation positions on the surfaces of both the substrate and epitaxial film.

ECCI feature size has been previously confirmed [27]. After the deposition of a 600 nm GaN film on this substrate and etching in the aforementioned KOH solution, the same region as that shown in Fig. 3(a) was then evaluated using SEM. A representative image of the dislocation-specific KOH etch pits is shown in Fig. 3(b). Each of the dislocations in the GaN film in Fig. 3(b) can be paired with one shown in the substrate in Fig. 3(a). The generation of additional threading dislocations during the growth of the GaN film was not observed in analogous micrographs of any samples.

The terrace width and step orientation varied only slightly from one region to another within the interior of the surface of each of the films investigated using AFM. (These results are in contrast to those acquired from the edges of the films and substrates, as described below.) Representative examples of this variation are indicated in the sample outline in Fig. 4(a) and shown in the corresponding micrographs of the surface of the 5 nm GaN(0001) film in Fig. 4(b)–(d). Similar variations were observed across the surfaces of the other films and the substrates on which they were grown. These results in tandem with the absence of a film/substrate interface indicate that the anisotropy and orientation of the grains within each substrate were reproduced in each of the associated films.

The tilts and twists between adjacent grains within each substrate resulted in the observed variations in terrace widths and step orientations, respectively. The degree of off-cut also influenced the terrace widths within all the grains. The regions containing the abnormally narrow terrace widths (or highly dense steps) in the GaN substrates corresponded to a local and larger effective off-cut angle on that specific grain than the average off-cut angle across the whole of the surface.

The existence of highly disoriented grains in the periphery of the GaN substrates was verified using orientation image microscopy (OIM). Fig. 5(a) shows the normal direction inverse pole figure map of approximately one-half of a 1 cm × 1 cm GaN

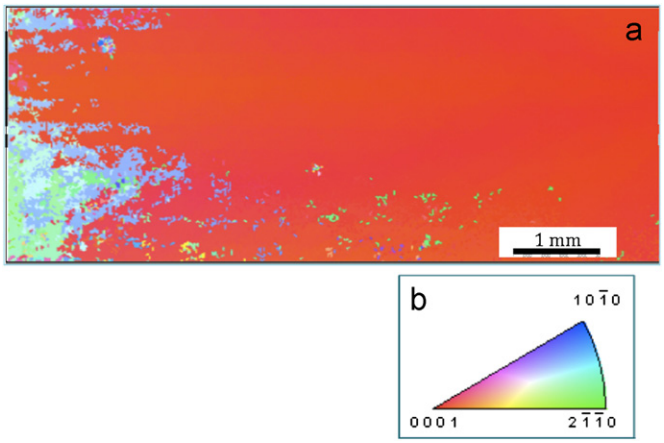

Fig. 5. (a) Normal direction inverse pole figure map of a representative GaN substrate. The color of each pixel in the map is determined by the orientation of the pixel area by reference to the inverse pole figure legend in (b). In the latter figure, each color denotes a crystallographic direction within a GaN grain when parallel to the sample surface normal direction. Much of the mapped area has the [0001] direction parallel to the sample surface normal. The bottom corner area reveals that the substrate contains grains having other crystallographic directions parallel to the substrate surface normal, and indicates polycrystallinity within the substrate. (For interpretation of the references to color in this figure legend, the reader is referred to the web version of this article.)

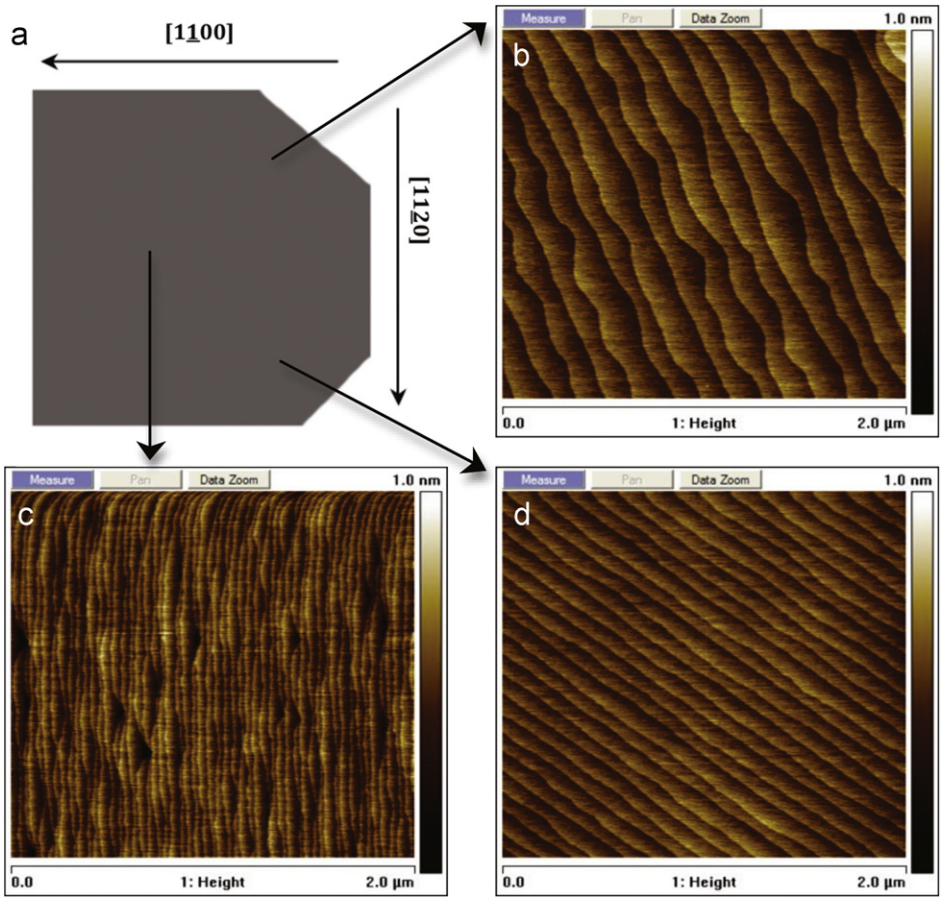

Fig. 4. (a) Outline of the total surface of a homoepitaxial 5 nm GaN film on GaN(0001) substrate. Arrows indicate the sites from which the AFM micrographs shown in (b)–(d) were acquired. The scanning conditions and the scanning direction of the instrument tip were the same for the acquisition of all images.

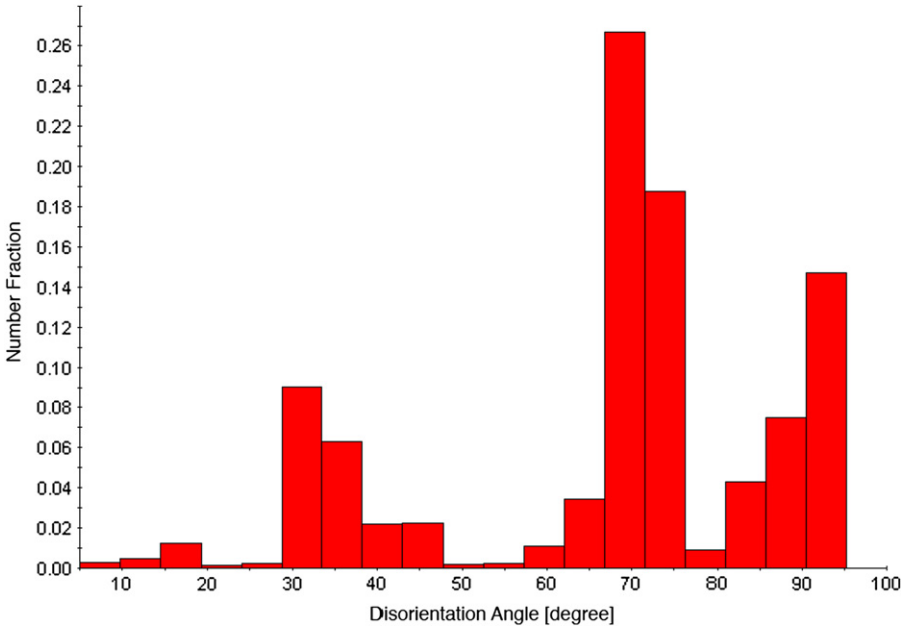

Fig. 6. Histogram of disorientation angles between adjacent grains in a GaN substrates used in this study. Using the criterion that the observation of a disorientation angle larger than 5° indicates two grains, the GaN substrates must be considered polycrystalline. Approximately 45% of the disorientation angles are ~70°, ~25% are ~90° and ~20% are 35°.

substrate representative of those used in this research. The legend for this figure is given in Fig. 5(b) where each color corresponds to a particular crystallographic direction within a GaN grain, if it is parallel to the normal direction in the sample reference frame. The former figure reveals the distribution of all the crystallographic directions that are parallel to the sample normal direction across the GaN substrate. To distinguish these results from those obtained using AFM of the very slightly disoriented grains, the criterion that a disorientation angle larger than 5° indicates another grain was established. A continuous area having colors that corresponds to a disorientation angle less than 5° is regarded as one grain, and the nominal diameter of this grain is on the order of mm. Under these criteria, much of the area of the substrate is normally oriented along the [0001] direction (shown in red). Additional grains with other crystallographic directions parallel to the substrate surface normal were observed around the edge of each substrate; an example of these grains located at the bottom left corner area of one of the substrates is shown in Fig. 5(a). The nominal diameters of these grains varied from several microns to hundreds of microns. It is worth noting that the 5° criterion allows the appearance of the slight variations of step orientation and terrace width observed in AFM from one site to another, within an as-defined grain, The distribution of the disorientation angles among *adjacent* grains is shown in Fig. 6. Approximately 25% of the disorientation angles are as high as 90°, ~45% are ~70° and ~20% are near 35°.

4. Conclusions

Polycrystalline homoepitaxial GaN(0001) films having a thickness range of 1–600 nm have been reproducibly grown using a specifically designed OMVPE process route that promoted step-flow growth and allowed reproduction of the surface microstructure of the CMP GaN substrates. Neither the formation of three-dimensional GaN islands at the film–substrate interface nor the generation of new threading dislocations in the GaN films were observed. The microstructures of the GaN films inferred from the micrographs of the surface acquired using AFM agree well with those obtained from high-resolution TEM, ECCI, and chemical etching. The variations in step orientation and terrace width observed via AFM in the interior areas of the surfaces of the films mimicked those observed on similar areas of the surfaces of the substrates and occurred as a result of twists and tilts, respectively, among adjacent grains. The grain orientation map across a representative GaN substrate and the companion histogram of disorientation angles between neighboring grains revealed that the substrate contained grains at the edge that were highly disoriented.

Acknowledgments

The authors would like to thank Department of Energy for financial support under the project contract number of DOE DEFC2607NT43229. Y.N. Picard recognizes financial support from the Army Research Office through project contract number W911NF1010309.

References

[1] P.Q. Miraglia, E.A. Preble, A.M. Roskowski, S. Einfeldt, R.F. Davis, Helical-type surface defects in GaN thin films epitaxially grown on GaN templates at reduced temperatures, Journal of Crystal Growth 253 (2003) 16–25.
[2] Z.J. Reitmeier, S. Einfeldt, R.F. Davis, X. Zhang, X. Fang, S. Mahajan, Sequential growths of AlN and GaN layers on as-polished 6H–SiC(0001) substrates, Acta Materialia 57 (2009) 4001–4008.
[3] Z.J. Reitmeier, S. Einfeldt, R.F. Davis, X. Zhang, X. Fang, S. Mahajan, Surface and defect microstructure of GaN and AlN layers grown on hydrogen-etched 6H–SiC(0001) substrates, Acta Materialia 58 (2010) 2165–2175.
[4] M.A. Moram, C.S. Ghedia, D.V.S. Rao, J.S. Barnard, Y. Zhang, M.J. Kappers, C.J. Humphreys, On the origin of threading dislocations in GaN films, Journal of Applied Physics 106 (2009) 073513–073519.
[5] A.M. Sanchez, M. Gass, A.J. Papworth, P.J. Goodhew, P. Singh, P. Ruterana, H.K. Cho, R.J. Choi, H.J. Lee, V-defects and dislocations in InGaN/GaN heterostructures, Thin Solid Films 479 (2005) 316–320.
[6] N. Sharma, P. Thomas, D. Tricker, C. Humphreys, Chemical mapping and formation of V-defects in InGaN multiple quantum wells, Applied Physics Letters 77 (2000) 1274–1276.
[7] H.K. Cho, J.Y. Lee, G.M. Yang, C.S. Kim, Formation mechanism of V defects in the InGaN/GaN multiple quantum wells grown on GaN layers with low threading dislocation density, Applied Physics Letters 79 (2001) 215–217.

[8] M. Shiojiri, C.C. Chuo, J.T. Hsu, J.R. Yang, H. Saijo, Structure and formation mechanism of V defects in multiple InGaN/GaN quantum well layers, Journal of Applied Physics 99 (2006) 073505–073506.
[9] A. Hangleiter, F. Hitzel, C. Netzel, D. Fuhrmann, U. Rossow, G. Ade, P. Hinze, Suppression of nonradiative recombination by V-Shaped pits in GaInN/GaN quantum wells produces a large increase in the light emission efficiency, Physical Review Letters 95 (2005) 127402.
[10] X.A. Cao, J.A. Teetsov, F. Shahedipour-Sandvik, S.D. Arthur, Microstructural origin of leakage current in GaN/InGaN light-emitting diodes, Journal of Crystal Growth 264 (2004) 172–177.
[11] A.R. Michael, M. Hadis, Luminescence properties of defects in GaN, Journal of Applied Physics 97 (2005) 061301.
[12] K. Leung, A.F. Wright, E.B. Stechel, Charge accumulation at a threading edge dislocation in gallium nitride, Applied Physics Letters 74 (1999) 2495–2497.
[13] D. Cherns, S.J. Henley, F.A. Ponce, Edge and screw dislocations as nonradiative centers in InGaN/GaN quantum well luminescence, Applied Physics Letters 78 (2001) 2691–2693.
[14] D. Xiao, K.W. Kim, J.M. Zavada, Envelope-function analysis of wurtzite InGaN/GaN quantum well light emitting diodes, Journal of Applied Physics 96 (2004) 723–728.
[15] X.H. Wu, P. Fini, E.J. Tarsa, B. Heying, S. Keller, U.K. Mishra, S.P. DenBaars, J.S. Speck, Dislocation generation in GaN heteroepitaxy, Journal of Crystal Growth 189–190 (1998) 231–243.
[16] V. Potin, P. Ruterana, G. Nouet, R.C. Pond, Morko, ccedil, H., Mosaic growth of GaN on (0001) sapphire: a high-resolution electron microscopy and crystallographic study of threading dislocations from low-angle to high-angle grain boundaries, Physical Review B 61 (2000) 5587.
[17] W. Qian, M. Skowronski, M. De Graef, K. Doverspike, L.B. Rowland, D.K. Gaskill, Microstructural characterization of alpha-GaN films grown on sapphire by organometallic vapor phase epitaxy, Applied Physics Letters 66 (1995) 1252–1254.
[18] R. Datta, M.J. Kappers, M.E. Vickers, J.S. Barnard, C.J. Humphreys, Growth and characterisation of GaN with reduced dislocation density, Superlattices and Microstructures 36 (2004) 393–401.
[19] Y.N. Picard, M.E. Twigg, J.D. Caldwell, C.R. Eddy Jr, M.A. Mastro, R.T. Holm, Resolving the Burgers vector for individual GaN dislocations by electron channeling contrast imaging, Scripta Materialia 61 (2009) 773–776.
[20] X. Xu, R.P. Vaudo, A. Salant, J. Malcarne, J.S. Flynn, E.L. Hutchins, J.A. Dion, G.R. Brandes, Growth and Characteristics of Freestanding Gallium Nitride Substrates, 〈www.cree.com/products/pdf/Free_Standing_Substrate_Characteristics.pdf〉.
[21] X. Xu, R.P. Vaudo, J. Flynn, J. Dion, G.R. Brandes, MOVPE homoepitaxial growth on vicinal GaN(0001) substrates, Physica Status Solidi (a) 202 (2005) 727–731.
[22] K. Tachibana, H. Nago, S.-y. Nunoue, Extremely smooth surface morphology of GaN-based layers on misoriented GaN substrates for high-power blue-violet lasers, Physica Status Solidi (c) 3 (2006) 1819–1822.
[23] F.A. Ponce, D.P. Bour, W. Gotz, N.M. Johnson, H.I. Helava, I. Grzegory, J. Jun, S. Porowski, Homoepitaxy of GaN on polished bulk single crystals by metalorganic chemical vapor deposition, Applied Physics Letters 68 (1996) 917–919.
[24] P.R. Daniels, E.A. Preble, T. Paskova, D. Hanser, Orientation control of bulk GaN substrates grown via hydride vapor phase epitaxy, in: Proceedings of the CS MANTECH Conference, Tampa, Florida, USA, 2009, p. 3.
[25] Z.J. Reitmeier, J.S. Park, W.J. Mecouch, R.F. Davis, In situ cleaning of GaN(0001) surfaces in a metalorganic vapor phase epitaxy environment, Journal of Vacuum Science & Technology A: Vacuum, Surfaces, and Films 22 (2004) 2077–2082.
[26] R.F. Davis, A.M. Roskowski, E.A. Preble, J.S. Speck, B. Heying, J.A. Freitas Jr., E.R. Glaser, W.E. Carlos, Gallium nitride materials—progress, status, and potential roadblocks, Proceedings of the IEEE 90 (2002) 993–1004.
[27] R.J. Kamaladasa, F. Liu, L.M. Porter, R.F. Davis, D.D. Koleske, G. Mulholland, K.A. Jones, Y.N. Picard, Identifying threading dislocations in GaN films and substrates by electron channeling, Journal of Microscopy, 〈http://onlinelibrary.wiley.com/doi/10.1111/j.1365-2818.2011.03538.x/abstract〉.
[28] G. Kamler, J.L. Weyher, I. Grzegory, E. Jezierska, T. Wosinski, Defect-selective etching of GaN in a modified molten bases system, Journal of Crystal Growth 246 (2002) 21–24.